Evaluating State Dependence and Subtype Selectivity of Calcium Channel Modulators in Automated Electrophysiology Assays

Yuri A. Kuryshev, Arthur M. Brown, Emir Duzic, and Glenn E. Kirsch

ChanTest Corporation, Cleveland, Ohio.

ABSTRACT

Voltage-gated Ca^{2+} channels play essential roles in control of neurosecretion and muscle contraction. The pharmacological significance of Ca_v channels stem from their identification as the molecular targets of calcium blockers used in the treatment of cardiovascular diseases, such as hypertension, angina, and arrhythmia, and neurologic diseases, such as pain and seizure. It has been proposed that state-dependent Ca_v inhibitors, that is, those that preferentially bind to channels in open or inactivated states, may improve the therapeutic window over relatively state-independent Ca_v inhibitors. High-throughput fluorescent-based functional assays have been useful in screening chemical libraries to identify Ca_v inhibitors. However, hit confirmation, mechanism of action, and subtype selectivity are better suited to automated patch clamp assays that have sufficient capacity to handle the volume of compounds identified during screening, even of modest sized libraries (≤ 500,000 compounds), and the flexible voltage control that allows evaluation of state-dependent drug blocks. IonWorks™ Barracuda (IWB), the newest generation of IonWorks instruments, provides the opportunity to accelerate the Ca_v drug discovery studies in an automated patch clamp platform in 384-well format capable of medium throughput screening and profiling studies. We have validated $hCa_v1.2$, $hCa_v2.1$, $hCa_v2.2$, and $hCa_v3.2$ channels assays on the IWB platform (population patch clamp mode) and demonstrated that the biophysical characteristics of the channels (activation, inactivation, and steady-state inactivation) obtained with the IWB system are consistent with known subtype-specific characteristics. Using standard reference compounds (nifedipine, BAY K8644, verapamil, mibefradil, and pimozide), we demonstrated subtype-selective and state- and use-dependent characteristics of drug–channel interactions. Here we describe the design and validation of novel robust high-throughput Ca_v channel assays on the IWB platform. The assays can be used to screen focused compound libraries for state-dependent Ca_v channel antagonists, to prioritize compounds for potency or to counter-screen for Ca_v subtype selectivity.

INTRODUCTION

Voltage-gated Ca^{2+}–selective channels play essential roles in the control of neurosecretion and muscle contraction. The channels have been categorized as L-, N-, P/Q-, R-, or T-type based on functional and pharmacological properties. Sequence similarity has identified three subfamilies Ca_v1, Ca_v2, and Ca_v3, where Ca_v1 and Ca_v3 correspond to L- and T-type, respectively. Ca_v2 encompasses N-, R-, and P/Q types. Each subtype contains a pore-forming α_1-subunit accompanied by auxiliary subunits (*e.g.*, $\alpha_2\delta$, β_{1-4}, and γ) that modify gating, subcellular trafficking, and drug binding characteristics.[1]

Development of drugs that act as calcium channel blockers has been successful for L-type channels in cardiovascular indications, for example, hypertension, heart failure, and atrial fibrillation. The success in this area has been due largely to state-dependent and use-dependent characteristics of the drug–channel interaction such that the inhibitory effect is most pronounced at partially depolarized membrane potential, thus preserving normal function.[2]

Another area of calcium channel drug development has focused on neurologic disorders, including pain and epilepsy. Cav2.2 (N-type) has been identified as a valid pain target that can be inhibited by the selective blocker ziconotide to relieve chronic pain.[3] However, recent development has centered on identifying state-dependent $Ca_v2.2$ inhibitors, which preferentially bind to channels in open or inactivated states that may improve the therapeutic window over relatively state-independent $Ca_v2.2$ inhibitors, such as ziconotide.[4] Antiepileptic calcium channel inhibitors are exemplified by ethosuximide, broadly selective blockers of T-type (Cav3.x) channels.[5] Another example is gabapentin, which inhibits Cav2.x trafficking through interaction with the $\alpha_2\delta_1$ auxiliary subunit and is approved for treatment of both seizures and pain.[6]

State- and use-dependent characteristics, and subtype selectivity of voltage-gated channels can be measured in a straightforward manner using patch clamp methods. Automated, high-throughput platforms are preferred in screening and profiling studies, but until recently, automated patch clamp instruments lacked the required levels of throughput and flexibility. Systems such as IonWorks™ Barracuda (IWB) that operate in a 384-well format can evaluate small chemical

 DOI: 10.1089/adt.2013.552

libraries in the range of 20,000–100,000 compounds. In the present study, we show that state dependence and subtype selectivity can be readily assessed in IWB assays in recombinant cell lines that stably express L-, N-, P/Q, or T-type calcium channels.

MATERIALS AND METHODS

Cell Lines

Stable cell lines expressing (under tetracycline induction) human $Ca_v1.2/\beta_2/\alpha_2\delta_1$ (Chinese hamster ovary [CHO]; *CACNA1C/CACNB2/CACNA2D1*), $Ca_v2.1/\beta_4/\alpha_2\delta_1$ (CHO; *CACNA1A/CACNB4/CACNA2D1*), $Ca_v2.2/\beta_3/\alpha_2\delta_1$ (CHO; *CACNA1B/CACNB2/CACNA2D1*), and $Ca_v3.2$ (HEK293; *CACNA1H*) ion channels were constructed as described previously.[7] CHO cells were maintained in Ham's F-12 CHO media supplemented with 10% fetal bovine serum, 100 U/mL of penicillin G sodium, 100 μg/mL of streptomycin sulfate, and the appropriate selection antibiotics. HEK293 cells were maintained in the Dulbecco's modified Eagle's medium/nutrient mixture F-12 (DMEM/F-12) supplemented with 10% fetal bovine serum, 100 U/mL of penicillin G sodium, 100 μg/mL of streptomycin sulfate, and 500 μg/mL of G418 as the selection antibiotic. For experiments, the cells were passed in a medium lacking selection antibiotics 2–4 days. Expression was induced with tetracycline 16–14 h before recording. Verapamil at 3 μM was included in the induction medium to avoid Ca^{2+} overload toxicity. Cell density was ~50%–70% confluent at the time of harvest; two 150-mm plates (~1.2×10^7 cells) were used per population patch clamp (PPC) experiment.

Cells were harvested by washing twice with 15–20 mL of Hank's Balanced Salt Solution (HBSS) and treatment with 5 mL of Accutase™ (Innovative Cell Technologies, San Diego, CA) solution for 20 (CHO cells) or 60 (HEK293 cells) minutes. Cells were resuspended in a 50-mL conical tube with addition of 10 mL of HBSS and triturated with a serological pipette to resuspend the cells and break up cell clusters. Cells were pelleted at 500 *g* for 2.5 min, the supernatant was removed, and the cell pellet was resuspended in 10 mL of HBSS. The cell suspension was centrifuged again at 500 *g* for 2.5 min and the supernatant removed. Finally, the cell pellet was resuspended in 5 mL of HEPES-buffered physiological saline (HB-PS).

Solutions and Electrophysiological Procedures

Chemicals used in a solution preparation were purchased from Sigma-Aldrich (St. Louis, MO) and were of ACS reagent grade purity or higher. Stock solutions of test articles were prepared in dimethyl sulfoxide (DMSO) and stored frozen. Each test article formulation was sonicated (Model 2510/5510; Branson Ultrasonics, Danbury, CT) at ambient room temperature for 20 min to facilitate dissolution. Test article concentrations were prepared fresh daily by diluting stock solutions into extracellular solutions (HB-PS buffer). The solution composition was 137 mM NaCl, 4 mM KCl, 7 mM $CaCl_2$, 1 mM $MgCl_2$, 10 mM HEPES, and 10 mM glucose, pH adjusted to 7.4 with NaOH. All test and control solutions contained 0.3% DMSO and 0.05% F-127. The test article formulations were prepared in 384-well compound plates using an automated liquid handling system (Cyclone, Caliper). The internal HEPES-buffered solution consisted of 90 mM CsF, 50 mM CsCl, 2 mM $MgCl_2$, 0.5 mM EGTA, and 10 mM HEPES, pH 7.2 adjusted with CsOH. A stock solution of amphotericin B was prepared in DMSO (30 mg/mL) and added to the solution at a final concentration of 100 μg/mL. An extracellular buffer was loaded into the PPC plate wells (11 μL/well) and a cell suspension was added into the wells (9 μL/well). After establishment of a whole-cell configuration (a 10-min perforation), membrane currents were recorded by on-board patch clamp amplifiers in IWB. The data acquisition frequency was 5 kHz. Inward peak current amplitudes were measured. Under these conditions, each assay was completed in 45 min, and 5–10 experiments could be conducted each day.

Data Analysis

Initial data acquisition and analyses were performed using the IWB system operation software (version 2.0.2; Molecular Devices Corporation, Union City, CA). Data were corrected for leak current. The decrease in current amplitude after test article application was used to calculate the percent block relative to control. Results for each test article concentration ($n=3$–4) were averaged, mean and standard deviation values were calculated and used to generate dose–response curves in XLfit add-in for Excel 2003 (Microsoft, Redmond, WA).

Drug effects were calculated as follows:

$$\%\text{Block} = \left[\frac{(1-I_{TA})}{I_{Baseline}}\right]\times 100\%,$$

where $I_{Baseline}$ and I_{TA} were the current amplitudes measured at baseline (before addition of a test article) and in the presence of a test article (or vehicle control), respectively.

If not specified, the data were corrected for run-down using the following equation:

$$\%\text{Block}' = 100\% - \left[(\%\text{Block} - \%\text{PC})\times\frac{100\%}{\%\text{VC} - \%\text{PC}}\right],$$

where %VC and %PC were the mean values of the current inhibition with the vehicle and positive controls, respectively; inhibition by saturating concentrations of nifedipine ($Ca_v1.2$) or mibefradil ($Ca_v2.1$, $Ca_v2.2$, $Ca_v3.2$) was used as %PC value.

The concentration–response data for inhibitors were fit to an equation of the following form:

$$\%\text{Block} = \frac{100\%}{1+([\text{Test}]/IC_{50})^N},$$

Table 1. Acceptance Criteria for Wells

Parameter	Acceptance criterion
R_{SEAL} (baseline)[a]	> 300 MΩ
Current amplitude (baseline)	> 0.2 nA
R_{SEAL} stability	< 50% decrease
Current stability	< 50% decrease in mean of vehicle control
Voltage clamp quality	Visual inspection

[a]Typical R_{SEAL} values ranged between 500 and 1,000 MΩ.

Table 2. Acceptance Criteria for 384-Well Population Patch Clamp Plate

Parameter	Acceptance criterion
Z′ factor	≥0.4
SW	≥2
Success rate	>80% accepted wells per PPC plate
IC_{50} for reference inhibitors	≤0.5 log from historical mean

SW, signal window; PPC, population patch clamp.

where [Test] was the concentration of test article, IC_{50} was the concentration of the test article producing half-maximal inhibition, *N* was the Hill coefficient, and %Block was the mean value of percentage of the current inhibited at each concentration of a test article. Nonlinear least square fits were solved with the XLfit add-in for Excel 2003 (Microsoft).

Acceptance Criteria

Individual well data were filtered according to the criteria listed in *Table 1* and the experiments were accepted based on the criteria listed in *Table 2*.

The Z′ factor and signal window (SW) in each experiment were calculated as follows:

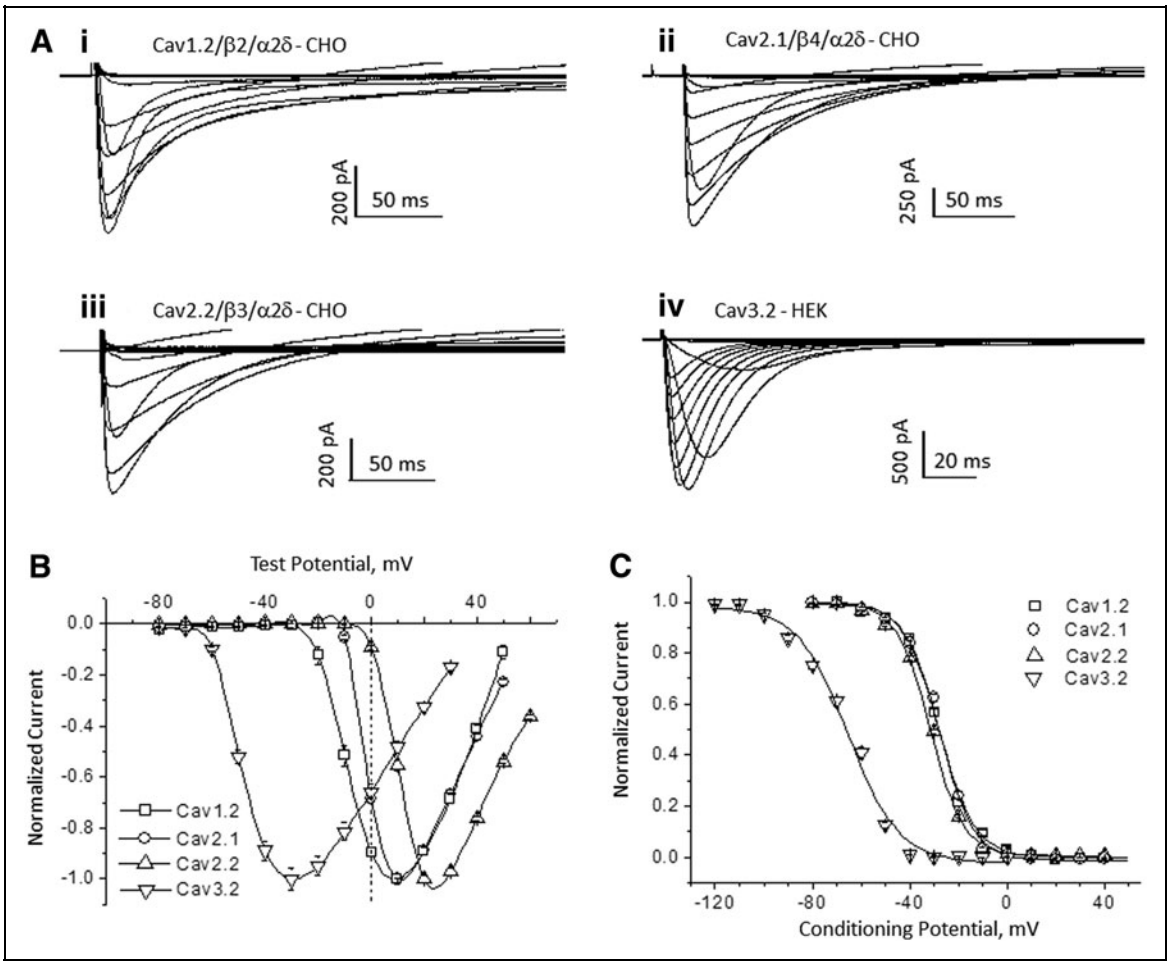

Fig. 1. Electrophysiological characteristics of Ca_v channels in IonWorks™ Barracuda. **(A, B)** Voltage-dependent activation of channels. Calcium current families, where 7 mM Ca^{2+} is the charge carrier: $Ca_v1.2$ **(i)**, $Ca_v2.1$ **(ii)**, $Ca_v2.2$ **(iii)**, and $Ca_v3.2$ **(iv)**. Currents were elicited by applying test pulses from −80 to +60 mV in 10 mV increments; the holding potential of −80 mV for $Ca_v1.2$ and −90 mV for other channels. In case of $Ca_v3.2$, a 500-ms conditioning voltage prepulse to −120 mV preceded each test pulse. The averaged current–voltage relationship is shown in **(B)** (mean ± SE; $n=16$). Superimposition of steady-state inactivation curves of Ca_v channels is illustrated in **(C)**. The currents were elicited by 400 ms test pulses, after 1-s, the conditioning prepulses (CPs) ranged from −120 to 50 mV (10 mV increments); the test pulse potentials were 10, 10, 30, and −30 mV for $Ca_v1.2$, $Ca_v2.1$, $Ca_v2.2$, and $Ca_v3.2$ channels, respectively.

$$Z' = 1 - \frac{3 \times \mathrm{SDVC} + 3 \times \mathrm{SDPC}}{\mathrm{ABS}(\mathrm{MeanVC} - \mathrm{MeanPC})},$$

$$\mathrm{SW} = \frac{(\mathrm{MeanPC} - 3 \times \mathrm{SDPC}) - (\mathrm{MeanVC} + 3 \times \mathrm{SDVC})}{\mathrm{SDVC}},$$

where MeanVC and SDVC are the mean and standard deviation values for a vehicle control, and MeanPC and SDPC are the mean and standard deviation values for a positive control.

RESULTS

We developed cell lines that express recombinant voltage-gated Ca^{2+} channels belonging to the L-, N-, P/Q-, and T-type classes: $hCa_v1.2$ ($\alpha_1C/\beta_2/\alpha_2\delta_1$), $hCa_v2.1$ ($\alpha_1A/\beta_4/\alpha_2\delta_1$), $hCa_v2.2$ ($\alpha_1B/\beta_3/\alpha_2\delta_1$), and $hCa_v3.2$ (α_1H), respectively; where $\alpha 1$ is the pore-forming subunit, and β_{1-4} and $\alpha_2\delta_1$ are auxiliary subunits. Based on the relatively depolarized voltage range required to activate the channels, $Ca_v1.2$, $Ca_v2.1$, and $Ca_v2.2$ are high-voltage-activated channels, whereas $Ca_v3.2$ is activated at more negative membrane potentials and classified as a low-voltage-activated channel. *Figure 1A* illustrates representative families of current traces for each channel recorded in IWB. Currents were evoked by voltage pulses that span the range from −80 to +60 mV in 10 mV increments. The current–voltage relationships (*Fig. 1B*) show the expected separation of voltage ranges between the high- and low-voltage-activated channels. Thus, $hCa_v1.2$, $hCa_v2.2$, and $hCa_v2.1$ show peak responses at positive membrane potentials, whereas $hCa_v3.2$ peaks at about −30 mV. All four channel subtypes display voltage-dependent inactivation during prolonged depolarization (*Fig. 1A*), as indicated by the return to baseline current. The voltage dependence of inactivation is plotted in *Figure 1C*. Steady-state inactivation curves fitted using the Boltzmann equation with half-inactivation ($h_{0.5}$) values were −65.8, −31.6, −27.4, and −26.7 mV for $Ca_v3.2$, $Ca_v2.2$, $Ca_v2.1$, and $Ca_v1.2$, respectively. Thus, as compared with the high-voltage-activated subtypes, inactivation of $Ca_v3.2$ was shifted nearly 40 mV toward more negative potentials. These results confirm that patch clamp recordings in the IWB platform can recapitulate the known voltage-dependent gating characteristics of these Ca^{2+} channel subtypes. Based on these results, we selected conditioning pulses that allow evaluation of state-dependent inhibition and test pulse potentials that would be expected to minimize the effect of uncompensated series resistance error.

The channel subtypes also are distinguished on the basis of their pharmacological properties. The pore-forming α_1 subunits confer selective sensitivity to most of the known activators and inhibitors (with the exception of gabapentin and pregabalin that bind the auxiliary $\alpha_2\delta$ subunit). In particular, $Ca_v1.2$ and other L-type channels are sensitive to dihydropyridine activators (*e.g.*, BAY K8644) and inhibitors (*e.g.*, nifedipine). Other high-voltage-activated and all low-voltage-activated Ca^{2+} channels have low sensitivity to dihydropyridines.[8] *Figure 2* illustrates $Ca_v1.2$ versus $Ca_v2.2$ differences in dihydropyridine sensitivity. Current traces recorded pre- (vehicle; baseline) and postcompound addition show that $Ca_v1.2$ currents (*Fig. 2A-i*) are completely blocked by 1 μM nifedipine and potentiated by 0.3 μM (*S*)-(−)-BAY K8644. By contrast, peak $Ca_v2.2$ (*Fig. 2A-ii*) current amplitude were unaffected by 1 μM nifedipine (compared with vehicle control records). Similarly,

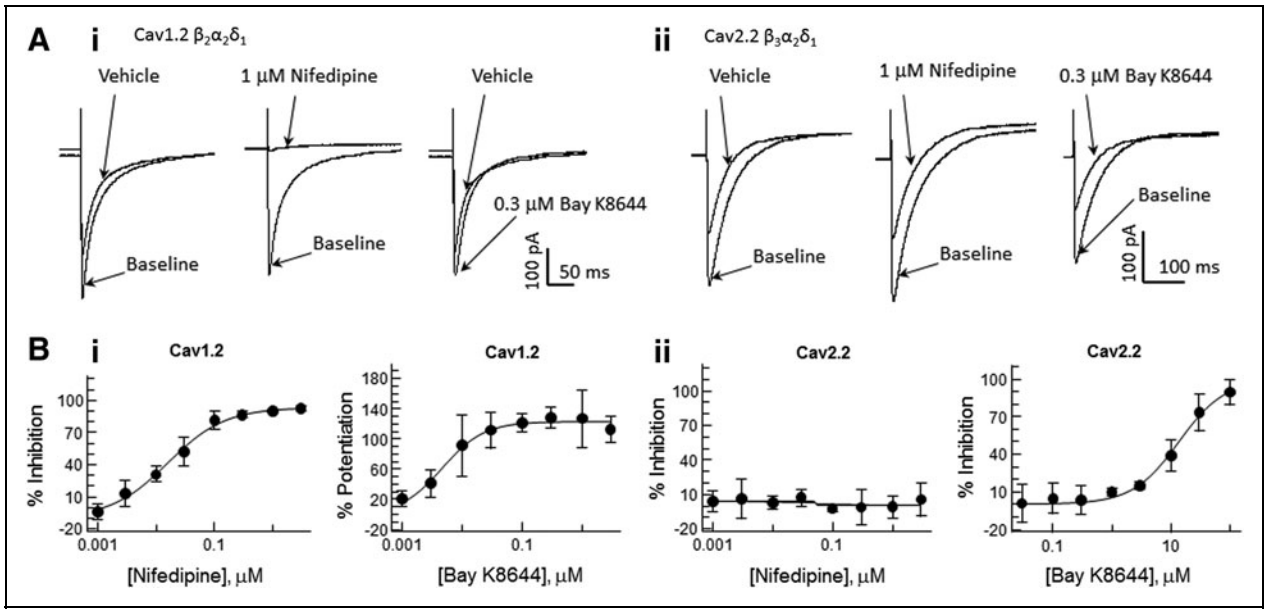

Fig. 2. Selectivity of pharmacological responses of Ca_v subtypes to dihydropyridine compounds. **(A)** Representative current traces illustrating effects of nifedipine and BAY K8644 on $Ca_v1.2$ **(i)** and $Ca_v2.2$ **(ii)** channels. The currents were elicited with test pulses to 10 mV ($Ca_v1.2$) and 30 mV ($Ca_v2.2$); the holding potential was −90 mV with 60-s CP to −50 mV. **(B)** Dose–response curves of the compounds effect on $Ca_v1.2$ **(i)** and $Ca_v2.2$ **(ii)** channels. Data presented as mean ± SD; $n = 4$. Data were fit to the Hill equation with coefficient in the range 0.6–2.0. Nifedipine inhibited $Ca_v1.2$ channels ($IC_{50} = 0.016$ μM) and had no effects on $Ca_v2.2$ channels. BAY K8644 produced twofold potentiation of $Ca_v1.2$ channels ($EC_{50} = 0.006$ μM), but inhibited $Ca_v2.2$ channel ($IC_{50} = 14.3$ μM).

$Ca_v2.1$ and $Ca_v3.2$ channels were insensitive to nifedipine at concentrations up to 3 μM (not shown). Conversely, BAY K8644, a dihydropyridine compound that potentiates the L-type channel current, increased the $Ca_v1.2$ channel at low nanomolar concentrations (EC_{50} = 6 nM), but produced nonspecific inhibition of all four channels at concentrations ≥10 μM. Nifedipine block of $Ca_v1.2$ and BAY K8644 block of $Ca_v2.2$ were concentration dependent (*Fig. 2B*) with apparent IC_{50} values of 23 nM and 13.6 μM, respectively.

To evaluate the pharmacological responses of Ca_v channels in the IWB platform, we tested a set of well-characterized reference inhibitors (diltiazem, nifedipine, verapamil, mibefradil, and pimozide) for use- and/or voltage-dependent inhibition. The assays were optimized by testing several different voltage protocols to obtain the best balance between sensitivity and success rate. Examples of results obtained with two different voltage protocols are illustrated in *Figure 3*. A simple two-test pulse protocol (*Fig. 3A*) demonstrated the use dependence of $Ca_v1.2$ inhibition with verapamil; the inhibitory potency detected by the second test pulse (TP2) was 3.5-times greater than that produced during the first test pulse (TP1). IC_{50} values were 35.3 and 9.1 μM, respectively, for TP1 and TP2. Similar results were obtained for diltiazem block of $Ca_v1.2$ and mibefradil block of $Ca_v2.2$ and $Ca_v3.2$ channels (not illustrated). In contrast, inhibition of $Ca_v1.2$ by nifedipine showed no use dependence in the two-test pulse protocol; the IC_{50} values were 0.59 and 0.57 μM, respectively, for the TP1 and TP2.

Because continuous (5–10 min) clamping of $Ca_v1.2$, $Ca_v2.1$, and $Ca_v2.2$ cells at holding potentials of −50 or −40 mV, as commonly done in native cells under voltage clamp,[9] resulted in extensive run down of the currents, we used conditioning depolarizing prepulses to evaluate voltage-dependent inhibition in the IWB platform (*Fig. 3B*). In this voltage protocol, $Ca_v1.2$ cells were held at −80 mV before stimulation. Test pulses were preceded by 50-s conditioning steps to −40 mV. The preconditioning enhanced the potency of $Ca_v1.2$

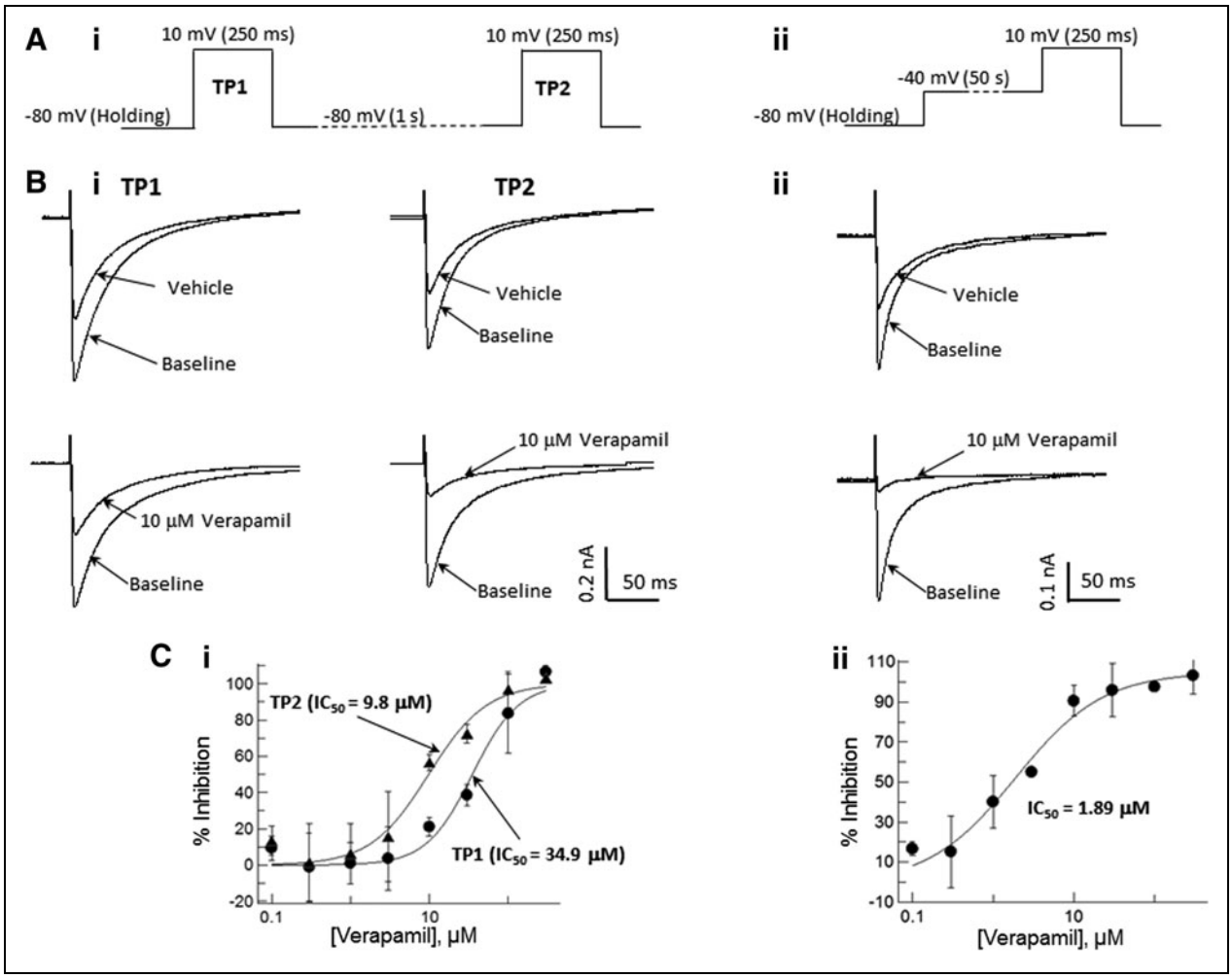

Fig. 3. Voltage and use dependence of $Ca_v1.2$ block by verapamil. **(A)** Examples of voltage protocols used for detection of use-dependent (two-pulse protocol; **i)** and voltage-dependent (preconditioning protocol; **ii)** effects of verapamil. **(B)** Representative current traces for the two-pulse **(i)** and preconditioning **(ii)** voltage protocols. **(C)** Dose–response curves for $Ca_v1.2$ inhibition by verapamil in the two-pulse **(i)** and preconditioning **(ii)** protocols.

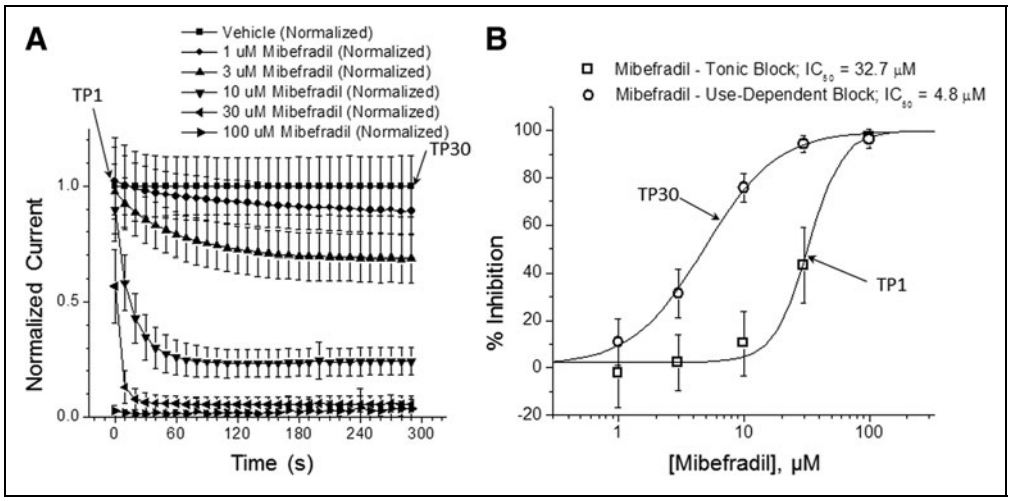

Fig. 4. Use-dependent block of $Ca_v2.2$ by mibefradil. **(A)** Time course of $Ca_v2.2$ inhibition with mibefradil during repetitive stimulation. The currents were elicited with test pulses to +20 mV from a holding potential −90 mV with 0.1 Hz frequency (30 stimulations in total); data were run down, corrected using time-matching vehicle control and presented as mean ± SD ($n = 4$ per concentration). **(B)** Dose–response curves for the first (TP1) and last (TP30) stimulation test pulses (mean ± SD). Mibefradil tonic block $IC_{50} = 32.7$ µM, use-dependent block $IC_{50} = 4.8$ µM.

inhibition compared with the two-test pulse protocol described above. IC_{50} values for the preconditioning protocol were 1.89, 0.013, and 2.43 µM, respectively, for verapamil, nifedipine, and diltiazem.

As an extension of the two-pulse voltage protocol, we evaluated use-dependent block augmentation by using stimulus patterns composed of repetitive test pulses. *Figure 4* illustrates an experiment in which $Ca_v2.2$ channels were stimulated by repetitive 400-ms test pulses to +20 mV from a holding potential −90 mV at frequency 0.1 Hz (30 test pulse train); mibefradil was added 5 min before stimulation by the TP1. Dose–response curves for the first (TP1) and last (TP30) test pulses were generated. Inhibition with mibefradil obtained at TP30 was about seven times more potent compared with the inhibition registered at TP1; IC_{50} values were 4.8 and 32.7 µM, respectively.

To utilize the high-throughput capabilities and increased stimulus flexibility in the IWB system, and to obtain more accurate prediction of both use- and voltage-dependent effects, we validated a multiple-mode voltage protocol that could be used with $Ca_v1.2$, $Ca_v2.1$, $Ca_v2.2$, and $Ca_v3.2$ channels. The voltage waveform of the protocol is shown in *Figure 5* and parameters specific for each Ca_v channel are provided in *Table 3*. IC_{50} values for reference compounds are presented in *Table 4*. The stimulus pattern consists of a combination of the two-pulse and use-dependent repetitive pulse patterns. As shown in the $Ca_v2.2$ example (*Fig. 5*), the first test pulse (TP1) consists of a brief depolarizing stimulus (+30 mV amplitude, 400 ms duration) preceded by a long, depolarizing conditioning pulse (−50 mV amplitude, 1 s duration) that would be expected to cause partial inactivation. TP1 is applied to both pre (baseline)- and post-compound application to assess the inactivation-sensitive component of block. The second test pulse (TP2) consists of the same depolarizing stimulus as TP1, preceded by a hyperpolarizing conditioning potential (−100 mV amplitude, 2-s duration). At baseline, TP2 evaluates maximum activation of channels from their resting state. After test compound application, TP2 can be used as a measure of tonic block of resting channels. An additional use-dependent block arising from repetitive activation of

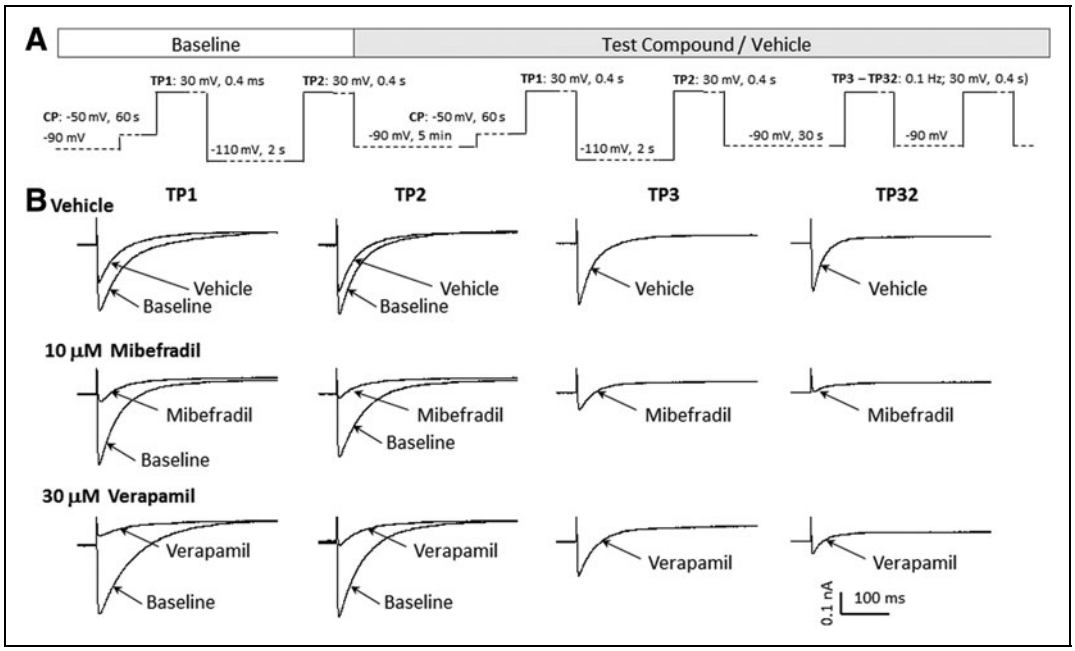

Fig. 5. Multiple mode voltage protocol for evaluation of voltage- and use-dependent block in Ca_v channels. **(A)** Optimized voltage protocol to detect use and voltage dependence of test compound interactions in Ca_v channels. **(B)** Representative $Ca_v2.2$ current traces elicited with the voltage protocols before (baseline) and after addition of vehicle, 10 µM mibefradil, and 30 µM verapamil.

Table 3. Multiple Mode Voltage Protocol Parameters

Ion channel	Holding potential (mV)	CP potential (mV)	CP duration (s)	TP potential (TP1–TP32, mV)	TP duration (TP1–TP32, ms)	TP frequency (TP3–TP32, Hz)
Cav1.2	−90	−50	60	10	250	0.1
Cav2.1	−90	−50	60	10	400	0.1
Cav2.2	−90	−50	60	30	400	0.1
Cav3.2	−90	−75	60	−30	200	1

CP, conditioning prepulse; TP, test pulse.

the channels is evaluated by TP3 to TP32, consisting of a train of brief depolarizing pulses (+30 mV amplitude, 400 ms duration, from −90 mV holding potential, delivered repetitively at 10-s intervals). It is noteworthy that TP3, the initial pulse in the train, is preceded by a 30-s conditioning interval at the holding potential (−90 mV) and provides an alternative index of tonic block of the resting state. Block augmentation (postcompound addition) beyond the level attained in the resting state (*i.e.*, use-dependent block) is measured by comparing peak current amplitudes, TP3 versus TP32, normalized to the effects of repetitive stimulation in channels exposed to vehicle alone. $Ca_v2.2$ current traces elicited by the multiple mode assay (*Fig. 5B*) illustrate the blocking characteristics of mibefradil and verapamil. Mibefradil shows use-dependent, but not inactivation-dependent block augmentation. By contrast, verapamil shows both inactivation- and use-dependent block amounting to an approximately threefold increase in block compared with tonic levels at −90 mV preconditioning, as illustrated in *Figure 6* that plots the concentration–response curves for each Ca_v channel. *Table 4* presents IC_{50} values for voltage- and use-dependent block in the multiple mode assay. In these experiments, calculation of the Z′ statistic for TP1, using reference antagonists (*Table 5*) gave values exceeding 0.5 in each case, indicative of a robust assay.[10]

DISCUSSION

Voltage-gated calcium (Ca_v) channels activate as a function of membrane potential such that the probability of opening increases with membrane depolarization, but with prolonged depolarization the channels transit to a closed, inactivated state that can be both voltage and calcium dependent. Thus, changes in membrane potential populate different conformational states (closed, open, or inactivated) of the channel. It is well known that a drug binding to Ca_v channels often shows state dependence such that the affinity of antagonist binding changes depending upon the channel conformation.[11]

The goal of this study was to develop patch clamp assays of recombinant calcium channels that take full advantage of the flexibility and throughput capabilities of the recently released IWB automated patch clamp system. We were able to optimize assays for state- and use-dependent blocks in four different human Ca_v subtypes using a standardized pulse protocol. It should be recognized that the standard protocol developed here provides a useful tool for evaluating Ca_v subtype selectivity and for identifying dynamic characteristics of compounds, but may not be ideal for screening every class of compounds. For instance, compounds that require long exposure time or show a tendency to adsorb to the apparatus may require lengthened preincubation times and multiple applications at the expense of decreasing the number of data points that can be acquired per day. Therefore, in screening programs that require a high volume of output and rapid turnaround, pilot studies that allow further optimization for the classes of compounds to be tested and for the desired characteristics of the actives may be necessary. Another major consideration in designing an appropriate protocol would be data reduction and analysis. Our standard protocol yields

Table 4. Pharmacology Summary: Reference Compound Potencies

Reference compound	$Ca_v1.2$			$Ca_v2.1$			$Ca_v2.2$			$Ca_v3.2$		
	Pre-pulse −50 mV	Pre-pulse −90 mV	0.1 Hz	Pre-pulse −50 mV	Pre-pulse −90 mV	0.1 Hz	Pre-pulse −50 mV	Pre-pulse −90 mV	0.1 Hz	Pre-pulse −75 mV	Pre-pulse −90 mV	1 Hz
Verapamil	6.5 ± 1.5	25.3 ± 5.2	5.3 ± 1.1	5.0 ± 1.1	22.1 ± 4.7	12.4 ± 3.6	13.1 ± 2.7	46.0 ± 8.7	17.8 ± 3.1	14.3 ± 3.3	21.2 ± 3.8	12.7 ± 1.8
Nifedipine	0.023 ± 0.007	0.085 ± 0.026	0.10 ± 0.013	> 3.0	> 3.0	> 3.0	> 3.0	> 3.0	> 3.0	> 3.0	> 3.0	> 3.0
BAY K8644	(0.006; 0.005)[a]	ND	ND	5.4 ± 0.9	24.8 ± 7.3	10.0 ± 2.6	(13.6, 14.3)	(54.7, 37.2)	(17.3, 16.1)	10.8 ± 1.9	11.5 ± 0.6	7.2 ± 0.7
Pimozide	> 30.0	27.8 ± 9.8	1 .9 ± 0.6	> 30.0	> 30.0	> 30.0	> 30.0	> 30.0	> 30.0	8.9 ± 3.6	7.2 ± 1.2	5.5 ± 1.3
Mibefradil	10.8 ± 3.10	16.1 ± 4.6	8.0 ± 1.8	6.5 ± 1.2	4.0 ± 1.1	2.2 ± 0.6	10.8 ± 1.3	8.4 ± 2.1	3.0 ± 0.2	3.30 ± 0.9	3.7 ± 1.0	2.0 ± 0.9

Data are mean ± SD IC_{50}s (in μM) from three to four experiments; where only two experiments were run, data from each experiment are listed.
[a]EC_{50}, BAY K8644 potentiated $Ca_v1.2$.
ND, not determined.

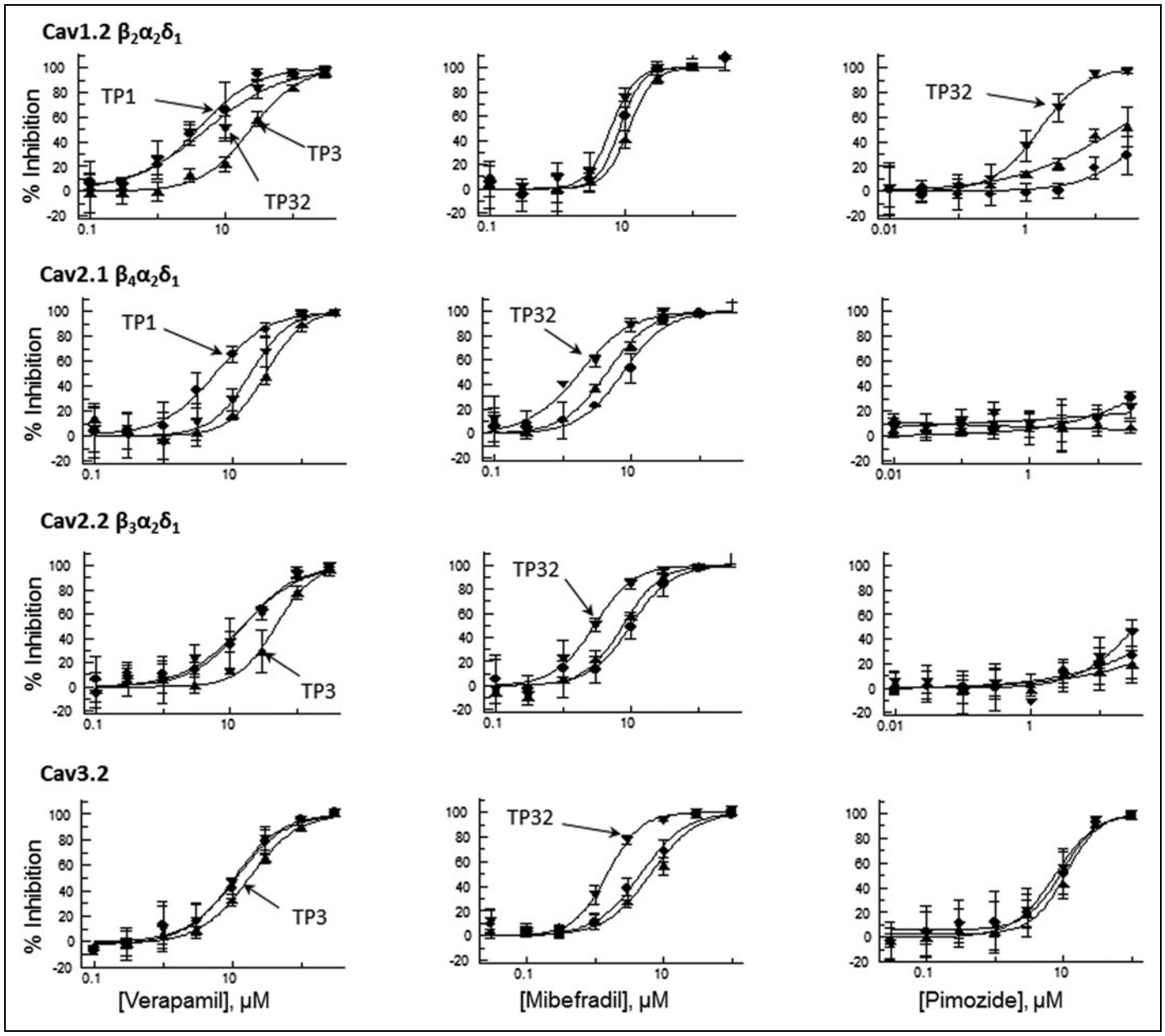

Fig. 6. Voltage- and use-dependent block of Ca_v channels by reference compounds recorded in the multiple mode protocol. Dose–response curves for verapamil, mibefradil, and pimozide, multiple mode assay protocol. The voltage protocol is shown in *Figure 5*; specific voltage parameters for each Ca_v channel are presented in *Table 3*. For each test compound and Ca_v channel target, three curves are superimposed: TP1 (circles)—the curve generated at the test pulse after the CP, TP3 (triangles)—the curve generated at the first test pulse from the holding potential, and TP32 (inverted triangles)—the curve generated at the last test pulse from the holding potential. IC_{50} values for the curves are presented in *Table 4*.

multiple endpoints that enable evaluation of state- and use-dependent block, but complicate the analysis and may not be essential for high-volume screening.

Our validation experiments yielded state-and use-dependent IC_{50} values of reference compounds in all four Ca_v channels, as presented in *Table 4*. These results highlight the differences between the channel subtypes. For instance, the dihydropyridine compounds nifedipine and antagonist, and BAY K8644, a potentiator, were effective in these roles only in $Ca_v1.2$. Other compounds showed less subtype selectivity. Thus, mibefradil, a use-dependent blocker that was originally described as a selective T-type channel antagonist and later shown to be a mixed T/L-blocker,[12] was observed in our experiments to be equipotent in the use-dependent evaluation of $Ca_v2.1$, $Ca_v2.2$, and $Ca_v3.2$. Nonetheless, mibefradil's use-dependent block was fourfold more potent in $Ca_v3.2$ versus $Ca_v1.2$, in agreement with published reports of $Ca_v3.2$ selectivity

Table 5. Assay Quality Parameters

	Ion channel											
	$Ca_v1.2$			$Ca_v2.1$			$Ca_v2.2$			$Ca_v3.2$		
Parameter	Pre-pulse −50 mV	Pre-pulse −90 mV	0.1 Hz (−90 mV)	Pre-pulse −50 mV	Pre-pulse −90 mV	0.1 Hz (−90 mV)	Pre-pulse −50 mV	Pre-pulse −90 mV	0.1 Hz (−90 mV)	Pre-pulse −75 mV	Pre-pulse −90 mV	1 Hz (−90 mV)
RD, %[a]	43.9 ± 1.4	N/A	N/A	26.1 ± 7.6	N/A	N/A	36.4 ± 4.5	N/A	N/A	28.8 ± 12.6	N/A	N/A
Z′	0.55 ± 0.09	0.56 ± 0.05	0.40 ± 0.06	0.57 ± 0.04	0.61 ± 0.06	0.46 ± 0.05	0.69 ± 0.03	0.64 ± 0.09	0.42 ± 0.09	0.65 ± 0.11	0.72 ± 0.03	0.64 ± 0.06
SW	4.0 ± 1.4	4.5 ± 0.6	3.3 ± 1.9	5.2 ± 1.2	5.9 ± 1.4	3.1 ± 0.8	6.4 ± 3.5	4.3 ± 1.0	3.0 ± 0.9	6.1 ± 2.2	10.9 ± 2.5	9.1 ± 2.9

Reference compounds for calculating Z′ and SW were verapamil ($Ca_v1.2$, $Ca_v2.1$, $Ca_v2.2$) or mibefradil ($Ca_v3.2$).
[a]RD was measured at TP1 in time-matched vehicle control wells.
RD, run down; TP1, test pulse 1.

over $Ca_v1.2$ reported by Martin *et al.* in manual patch clamp experiments.[13] However, our $Ca_v3.2$ IC_{50} value obtained with −90 mV prepulse (*Table 4*) was approximately sixfold higher than that reported by Martin *et al.*[13] The use dependence of mibefradil may account for this discrepancy. As is typical in manual patch clamp, the onset of block was evaluated by repetitive stimulation at 0.1 Hz until a steady-state effect was observed,[13] allowing cumulative use-dependent block, whereas in the IWB assay, stimulation was performed only once after exposure to the test compound for a fixed interval. Nonetheless, in IWB, by stimulating with a brief high-frequency train, we were able to achieve an IC_{50} value of 2.0 (*Table 4*, $Ca_v3.2$, 1 Hz stimulus frequency) similar to that observed in manual patch clamp.[13] This comparison of manual and automated patch clamp highlights the importance of recognizing the limitations of automated platforms and developing procedures that accommodate differences in the blocking kinetics and state-dependent characteristics of test compounds, as noted by others previously in $Ca_v2.2$ assays.[14]

Pimozide also has been described as a T-type channel inhibitor[15] and our evaluation of tonic block is consistent with this characterization. However, we found that pimozide's selectivity for $Ca_v3.2$ over $Ca_v1.2$ disappeared in the use-dependent assay, which gave IC_{50} values of 4.6 and 1.6 μM, respectively, in the two channel subtypes. As expected from the literature,[16] we found that verapamil was relatively nonselective. It showed a twofold to fivefold increase in potency for state-dependent block in the high-voltage-activated subtypes and state-independent block of the low-voltage-activated channel ($Ca_v3.2$).

Several studies of Ca_v channels in automated patch clamp have been published recently. Most notably, IonWorks Quattro (IWQ, the predecessor to IWB) has been used in $Ca_v1.2$ recording with results comparable to those described here. For instance, Morton and Main[17] reported a verapamil IC_{50} value of 3.3 μM (at a holding potential of −60 mV), similar to the 4.3 μM IC_{50} value reported here (*Table 4*, prepulse −50 mV, holding potential, −90 mV). Interestingly, Cao *et al.*[18] also reported a verapamil IC_{50} value of 4.0 μM, but at a holding potential of −90 mV, whereas we observed a marked decrease in potency (IC_{50} = 24.2 μM, *Table 4*, prepulse and holding potential, −90 mV) under these conditions. This discrepancy may reflect the discontinuous voltage clamp characteristic of IWQ, which allows cells to be depolarized between voltage clamp recordings. Therefore, the continuous voltage clamp feature of IWB may be particularly important for characterizing the state and voltage dependence of Ca_v inhibitors.

Our $Ca_v1.2$ results (verapamil IC_{50} = 4.2 μM and nifedipine IC_{50} = 0.016 μM, *Table 4*) also can be compared with data obtained in gigaohm seal automated instruments such as PatchXpress® (Molecular Devices Corporation), where IC_{50} values of 15 and 0.016 μM, respectively, were obtained for verapamil and nifedipine.[19]

In conclusion, we have demonstrated that the advanced capabilities of a high-throughput automated patch clamp, including flexible voltage stimulation patterns, continuous voltage clamp, and rapid throughput, provide a suitable platform to support quantitative drug evaluation of potency, state and use dependence, and subtype selectivity in the therapeutically important voltage-gated Ca^{2+} channel family.

ACKNOWLEDGMENTS

We would like to thank Zhiqi Liu and Hung Lee (ChanTest Corporation) for their assistance in cell line development and IWB validation.

DISCLOSURE STATEMENT

No competing financial interests exist.

REFERENCES

1. Catterall WA, Perez-Reyes E, Snutch TP, Striessnig J: International Union of Pharmacology. XLVIII. Nomenclature and structure-function relationships of voltage-gated calcium channels. *Pharmacol Rev* 2005;57:411–425.
2. Triggle DJ: Drug targets in the voltage-gated calcium channel family: why some are and some are not. *Assay Drug Dev Technol* 2003;1:719–733.
3. Snutch TP: Targeting chronic and neuropathic pain: the N-type calcium channel comes of age. *NeuroRx* 2005;2:662–670.

4. McGivern JG, McDonough SI: Voltage-gated calcium channels as targets for the treatment of chronic pain. *Curr Drug Targets CNS Neurol Disord* 2004;3:457–478.
5. Gomora JC, Daud AN, Weiergräber M, Perez-Reyes E: Block of cloned human T-type calcium channels by succinimide antiepileptic drugs. *Mol Pharmacol* 2001;60:1121–1132.
6. Field MJ, Hughes J, Singh L: Further evidence for the role of the $\alpha_2\delta$ subunit of voltage dependent calcium channels in models of neuropathic pain. *Br J Pharmacol* 2000;131:282–286.
7. Wible BA, Kuryshev YA, Smith SS, Liu Z, Brown AM: An ion channel library for drug discovery and safety screening on automated platforms. *Assay Drug Dev Technol* 2008;6:765–780.
8. Doering CJ, Zamponi GW: Molecular pharmacology of high voltage-activated calcium channels. *J Bioenerg Biomembr* 2003;35:491–505.
9. Sanguinetti MC, Kass RS: Voltage-dependent block of calcium channel current in the calf cardiac Purkinje fiber by dihydropyridine calcium channel antagonists. *Circ Res* 1984;55:336–348.
10. Zhang JH, Chung TD, Oldenburg KR: A simple statistical parameter for use in evaluation and validation of high throughput screening assays. *J Biomol Screen* 1999;4:67–73.
11. Hondeghem LM, Katzung BG: Antiarrhythmic agents: the modulated receptor mechanism of action of sodium and calcium channel-blocking drugs. *Annu Rev Pharmacol Toxicol* 1984;24:387–423.
12. Mehrke G, Zong XG, Flockerzi V, Hofmann F: The Ca^{2+}-channel blocker Ro 40–5967 blocks differently T-type and L-type Ca^{2+} channels. *J Pharmacol Exp Ther* 1994;271:1483–1488.
13. Martin RL, Lee JH, Cribbs LL, Perez-Reyes E, Hanck DA: Mibefradil block of cloned T-type calcium channels. *J Pharmacol Exp Ther* 2000;295:302–308.
14. Swenson AM, Niforatos W, Vortherms TA: An automated electrophysiological assay for differentiating Cav2.2 inhibitors based on state dependence and kinetics. *Assay Drug Dev Technol* 2012;10:542–550.
15. Santi CM, Cayabyab FS, Sutton KG, *et al.*: Differential inhibition of T-type calcium channels by neuroleptics. *J Neurosci* 2002;22:396–403.
16. Lacinová L: Voltage-dependent calcium channels. *Gen Physiol Biophys* 2005;24 Suppl 1:1–78.
17. Morton MJ, Main MJ: Use of escin as a perforating agent on the IonWorks Quattro automated electrophysiology platform. *J Biomol Screen* 2013;18:128–134.
18. Cao X, Lee YT, Holmqvist M, Lin Y, *et al.*: Cardiac ion channel safety profiling on the IonWorks Quattro automated patch clamp system. *Assay Drug Dev Technol* 2010;8:766–780.
19. Balasubramanian B, Imredy JP, Kim D, *et al.*: Optimization of $Ca_v1.2$ screening with an automated planar patch clamp platform. *J Pharmacol Toxicol Methods* 2009;59:62–72.

Address correspondence to:
Glenn E. Kirsch, PhD
ChanTest Corporation
14656 Neo Parkway
Cleveland, OH 44128

E-mail: gkirsch@chantest.com

Abbreviations Used

CHO = chinese hamster ovary
CP = conditioning prepulse
DMEM/F-12 = Dulbecco's modified Eagle's medium/nutrient mixture F-12
DMSO = dimethyl sulfoxide
$h_{0.5}$ = half-inactivation
HB-PS = HEPES-buffered physiological saline
HBSS = Hank's Balanced Salt Solution
$hCa_v1.2$ = human $Ca_v1.2$
$hCa_v2.1$ = human $Ca_v2.1$
$hCa_v2.2$ = human $Ca_v2.2$
$hCa_v3.2$ = human $Ca_v3.2$
HEK = human embryonic kidney
IWB = IonWorks™ Barracuda
IWQ = IonWorks Quattro
PPC = population patch clamp
SW = signal window
TP1 = first test pulse
TP2 = second test pulse
TP30 = last test pulse